Hindawi
International Journal of Photoenergy
Volume 2017, Article ID 3106734, 15 pages
https://doi.org/10.1155/2017/3106734

Research Article

Simulation and Practical Implementation of ANFIS-Based MPPT Method for PV Applications Using Isolated Ćuk Converter

Abdullah M. Noman, Khaled E. Addoweesh, and Abdulrahman I. Alolah

Electrical Engineering Department, King Saud University, Riyadh, Saudi Arabia

Correspondence should be addressed to Abdullah M. Noman; anoman@ksu.edu.sa

Received 12 August 2017; Revised 27 October 2017; Accepted 12 November 2017; Published 21 December 2017

Academic Editor: Tariq Iqbal

Photovoltaic (PV) module behavior is not linear in nature with respect to environmental conditions and hence exhibits nonlinear PV curves. There is only a single point in the nonlinear PV curve at which the power is maximum. Therefore, special methods have been proposed to track this maximum power point (MPP). This paper proposed an intelligent method for MPP tracking (MPPT) based on adaptive neuro-fuzzy inference system (ANFIS) controller. The proposed system consists of a PV module connected to a DC-DC isolated Ćuk converter and load. A MATLAB/SIMULINK-based MPPT model is built to test the behavior of the proposed method. The proposed method is tested under different weather scenarios. Simulation results exhibit the successful tracking of the proposed method under all ambient conditions. Comparison of the tracking behavior of the proposed method with the perturb and observe method is also presented in the simulation results. In addition, a 220 W prototype with the help of dSPACE 1104 data acquisition system is built and tested under practical weather conditions on a sunny day as well as on a cloudy day. Experimental results are presented to verify the effectiveness of the proposed method. These results exhibit satisfactory performance under different practical weather conditions.

1. Introduction

Recently, the energy demand in the world is noticeably growing due to the fast growth in the population and economy. Natural gas, coal, and crude oil are the main current fossil fuels, which are used to supply world energy. In the later years, irritation about energy crisis has been increased. Fossil fuels have been started to be gradually depleted. On the other hand, concern about the fossil fuel exhaustion and other environmental problems such as global warming caused by conventional power generation have been increased. It is a global challenge to generate a secure, available, and reliable energy and at the same time reduce the greenhouse gas emission [1]. One of the most effective and most suitable solution to meet the worldwide energy requirements is the renewable energy resources. Renewable energy can solve these problems simultaneously since they are green, clean, environment friendly, and are sustainable.

There are many sources of renewable energy such as solar energy and wind energy. Photovoltaic (PV) system has taken a great attention and appears to be the most promising renewable energy source since it is a clean, maintenance-free, pollution-free, and not a noisy source [1, 2]. However, two important factors limit the implementation of photovoltaic systems: high installation cost and low efficiency of energy conversion [1]. The behavior of the PV module is nonlinear in nature and hence exhibits nonlinear PV curves. There exists only a unique point of maximum power in each PV curve, which needs special techniques called maximum power point tracking (MPPT) techniques to track it. Therefore, MPPT can be used to increase the system efficiency by fully utilizing the PV modules. Many methods have been reported in the literature for tracking the maximum power point [2]. Open circuit voltage method search for the MPP based on the relationship between the open circuit voltage V_{oc} and the voltage at maximum power V_{MPP} of the PV

module under varying solar radiation and temperature levels. This relationship is almost linear where the voltage at maximum power V_{MPP} equals the open circuit voltage V_{oc} multiplied by a constant [3–5]. The constant depends on the characteristic of the PV module. The value of this factor is reported to be between 0.71 and 0.78 [4]. The common value of this constant is about 0.76 (within ±2%) [5]. In order to implement the open circuit voltage method, the PV modules must be interrupted with a certain frequency to measure the output voltage of the PV modules. Although this method is simple, choosing the value of the constant is difficult. On the other hand, the power losses are high due to frequently interrupting the system [5].

Short circuit current method results from the fact that the relationship between the current at maximum power point I_{MPP} and the short circuit current of the PV module I_{sc} is almost linear where the current at maximum power I_{MPP} approximately equals the short circuit current I_{sc} multiplied by a constant [6]. The constant depends on the characteristic of the PV module. The main drawback of the open circuit voltage method and the short circuit current method is the power losses due to measuring V_{oc} and I_{sc}, and the maximum power point is never perfectly matched [6].

Perturbation and observation (P&O) method is an alternative method to obtain the maximum power point of the PV module. P&O method is the widely used technique to track MPP. It perturbs the operating point and observes the difference in power. It measures the voltage and current and calculates the power of the PV module. Then it perturbs the voltage to encounter the change direction. If power difference is positive, the direction of perturbation remains the same; otherwise, it is reversed. However, this method suffers from slow tracking speed and high oscillations around MPP [2–5]. Figure 1 shows the flowchart of the P&O MPPT algorithm.

Introducing a high efficient MPPT controller can help in decreasing the total cost of the PV systems since 7% of the initial PV system cost is spent on the MPPT controller and inverter [7]. Therefore, researchers are focusing on proposing high efficient MPPT techniques. The use of intelligent techniques has been increased over the last decade since they are simple, deal with imprecise inputs, does not need an accurate mathematical model, and can handle nonlinearity [8]. Artificial intelligence-based techniques such as the fuzzy logic controller (FLC), artificial neural networks (ANNs), and adaptive neuro-fuzzy inference systems (ANFIS) can be used as a controller to extract the maximum power that the PV modules capable of producing under changing weather conditions. This is because they have the advantages such as they are robust, relatively simple to design, and they do not require the knowledge of an exact model [8, 9].

The fuzzy logic controller was applied in designing different MPPT controllers [7, 8, 10–16]. They apply a set of linguistic rules to obtain the required duty cycle. The input variables of the fuzzy logic controller differ from one configuration to another. In [11–14], the input variables to the FLC are the error (E) and the change in error (ΔE). The error can be calculated as the change in the power to the change in the voltage of the PV module ($\Delta P/\Delta V$). The output variable from the FLC is the duty cycle. In other configurations, the change in the PV current instead of using the change in the PV voltage is used to calculate the error as in [15].

Noman et al. [17] proposed an algorithm-based FLC to achieve tracking the maximum power of the PV module under changing the weather conditions. The inputs of the FLC are the change in the voltage of the PV module (ΔV) and the change in the power of the PV module (ΔP). The output from FLC is ΔU which corresponds to the modulation signal, which is applied to the PWM modulator in order to produce the switching pulses to drive the MOSFET of the DC-DC buck-boost converter.

Many configurations have proposed to use ANNs for MPPT purpose. As mentioned above, the PV module is nonlinear in nature. Therefore, ANNs can solve this nonlinear problem without the need for a mathematical model. Ocran et al. [18] proposed an MPPT-based ANNs for solar electric vehicles. The input variables are the open circuit voltage (V_{oc}) and PV cell temperature (T_{PV}) while the output variable is the voltage at maximum power point (V_{MPP}). However, measuring the open circuit voltage needs interrupting the circuit, and consequently, a power loss occurs. Ramaprabha and Mathur [19] proposed a genetic algorithm-optimized ANNs for MPPT. The ANN was trained offline using GA-optimized data to obtain V_{MPP} under changing weather conditions. The main drawback of this configuration is the need for solar radiation sensor, which increases the MPPT system cost.

Recently, much research has been devoted to use adaptive neuro-fuzzy inference systems (ANFIS) for tracking the maximum power of PV modules. ANFIS is actually fuzzy inference system optimized by neural networks. In addition, ANFIS can generate the fuzzy rules automatically. Various ANFIS-based MPPT methods have been proposed to achieve MPPT [20–24]. The input variables and the output variables are different from one configuration to another. The input variables in [20] are the change in the PV voltage (ΔV_{PV}) and the change in the PV power (ΔP_{PV}), while the output variable is the duty cycle. On the other hand, the input variables to the ANFIS in [22] are the open circuit voltage (V_{oc}) and the short circuit current (I_{sc}), while the output variable is the voltage at maximum power (V_{MPP}). The disadvantage of this method is that the need for interrupting the PV system to measure the open circuit voltage and need to short circuit the PV module terminals to measure the short circuit current, which finally increases the system losses. Some other papers use the solar radiation and temperature as input variables, and the output variable is the voltage at maximum power (V_{MPP}) or the maximum power itself (P_{MPP}) [21, 23, 24]. However, measuring irradiance level by solar radiation sensor is not the exact solar radiation incident on the PV module since the aging of the PV modules as well as the partial shading is not taken into considerations. In addition, the solar radiation sensor is expensive which increases the MPPT total cost.

The ANFIS-based MPPT techniques are very accurate because they track the maximum power point without the need to interrupt the circuit or short circuit the PV module terminals or oscillating around MPP as conventional MPPT algorithms. However, the proposed techniques in the

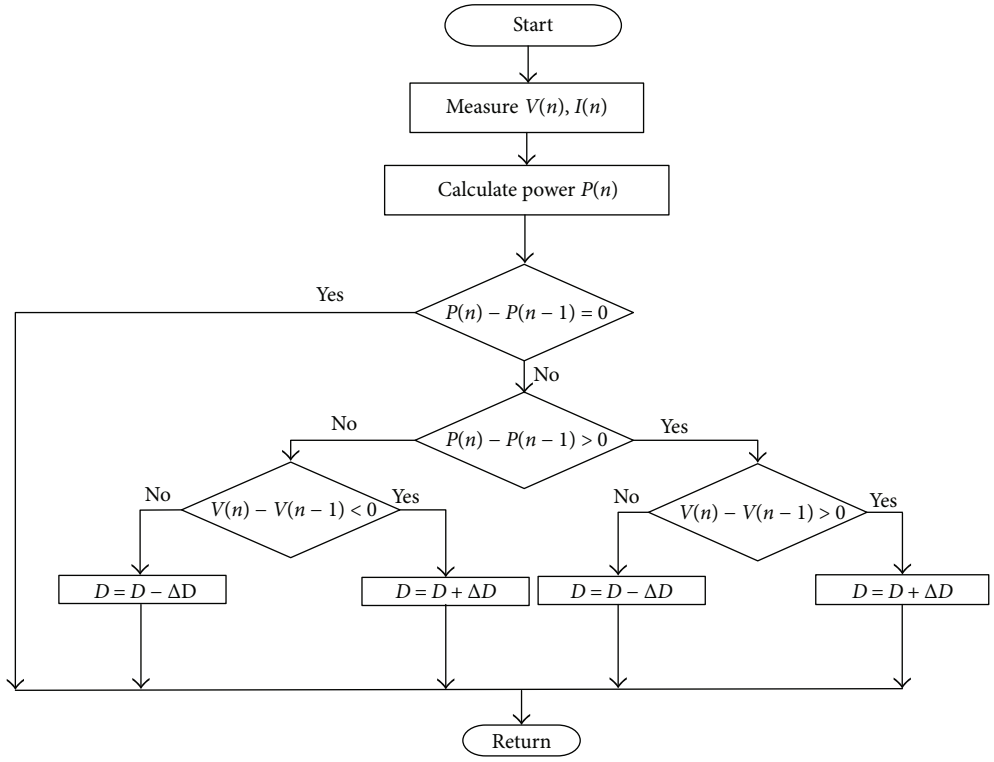

Figure 1: The flowchart of the P&O algorithm.

literature have some limitations since some of them need solar radiation sensor, which is expensive and does not estimate the exact incident solar radiation as mentioned above. In addition, some of the proposed ANFIS-based MPPT techniques measure V_{oc} and/or I_{sc} which increase the system losses. This paper presents a new MPPT method based on ANFIS to achieve maximum power point tracking. The proposed method depends on measuring the PV voltage (V_{PV}), the PV current (I_{PV}), and the PV cell temperature (T_{PV}) as input variables to the controller. It is known that there are some areas in the characteristic chart of the PV module at which the PV curves are overlapped to each other, especially under changing the temperature. These areas are located to the left of MPP and in the intersection points of PV curves (under constant solar radiation and changing temperature). If the MPPT controller starts tracking in these areas, the controller may be confused to track the current PV curve, especially if the input variables to the controller are not enough to make the right decision. Therefore, putting the PV cell temperature as another input variable to the ANFIS, the controller will not be confused to determine which PV curve where the measured temperature is belonging to, and hence the tracking will be more accurate and faster. In addition, the isolated Ćuk converter is used in this paper which is the first paper to use this type of converters. The isolated Ćuk converter has many advantages compared to the other isolated DC-DC converters as will be seen in later sections. The isolated Ćuk converter model and the performance of the ANFIS method are evaluated by MATLAB/SIMULINK environment. In addition, an experimental setup was established to verify the proposed MPPT method practically. DSPACE 1104 real-time data acquisition system is used in the implementation of the MPPT hardware setup.

2. System Modeling

2.1. Modeling of Photovoltaic Module. PV module essentially converts the incident light into electrical current when a load is connected to its terminals. Modeling the PV module requires first to model the photovoltaic cell. The electrical equivalent circuit of the PV cell is shown in Figure 2. As shown in this figure, the current source represents the amount of electron flow due to solar radiation incident on the PV cell. The diode represents the *PN* junction of the PV cell. There are two resistances: series resistance and parallel resistance. Series resistance accounts for the losses in the current path due to the metal grid, contacts, and current collecting bus. On the other hand, the parallel resistance accounts for the loss associated with a small leakage of current through a resistive path in parallel with the intrinsic device.

From Figure 2, the output current delivered to the load can be expressed as [25, 26]

$$I = I_{PV} - \underbrace{I_O\left(e^{q(V+IR_S)/nN_sKT_a} - 1\right)}_{I_D} - \underbrace{\frac{V_D}{R_P}}_{I_{R_P}}, \quad (1)$$

where I is the output current of the PV module (A); I_{PV} is the current source of the PV module by solar irradiance (A); I_D is

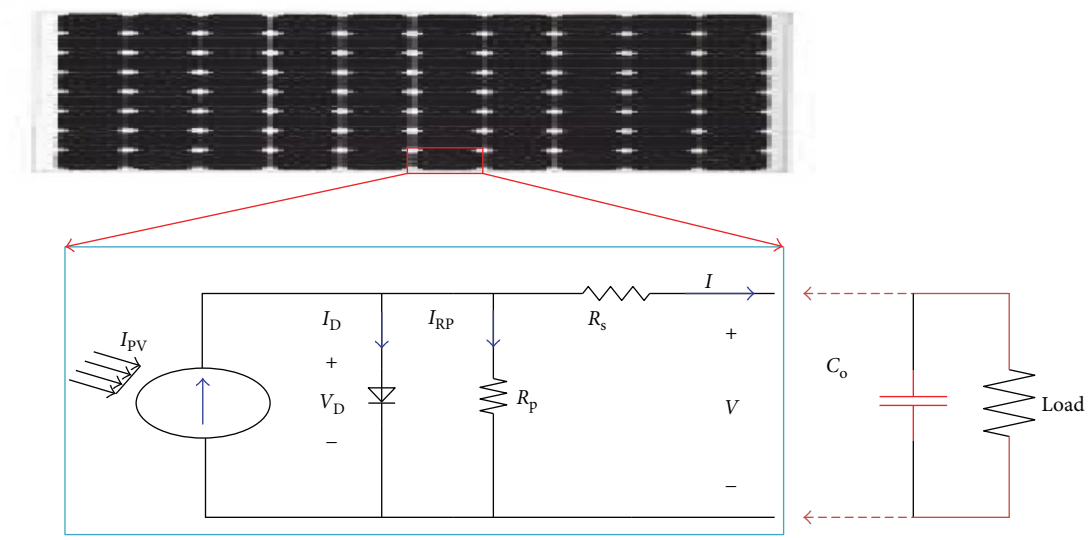

Figure 2: Equivalent circuit of PV cell simulation.

the diode current (A); I_{R_p} is the current flow to the parallel resistance R_P (A); I_o is the reverse current of a diode (A); N_S is the number of series cells in the PV module; n is the ideality factor of the diode ($n = 1\sim2$); q is the electric charge of an electron ($1.6 \times e^{-19}c$); k is the Boltzmann's constant (1.38×10^{-23} J/K); and T is the absolute temperature of the solar cell (K).

The current generated by the incident solar radiation, also called short circuit current (I_{sc}), at a given temperature (T_a) can be given as [25, 26]

$$I_{PV} = I_{scn}(1 + a(T_a - T_n))\frac{G}{G_n}, \quad (2)$$

where I_{scn} is the short circuit current at normal conditions ($T_n = 298$ K), $G_n = 1000$ W/m^2, T_a is the given temperature (K), a is the temperature coefficient of I_{sc}, and G is the given solar radiation (W/m^2).

The reverse saturation current of diode (I_o) at the normal conditions is given as [25, 26]

$$I_{on} = \frac{I_{scn}}{qV_{ocn}/e^{nN_skT_n} - 1}, \quad (3)$$

where V_{ocn} is the open circuit voltage of the PV module at normal conditions. The reverse saturation current at a given cell temperature (T_a) can be expressed as [26]

$$I_o = I_{on}\left(\frac{T_a}{T_n}\right)^{(3/n)} e^{-qE_g/nK(1/T_a - 1/T_n)}. \quad (4)$$

The PV module model number HIT-N220A01 is used in this paper. The PV module parameters under the standard conditions (1000 W/m^2, 298 K) are listed in Table 1. The PV module is simulated using MATLAB software. Figure 3 shows the simulated PV curves of the PV module under changing solar radiation from 200 W/m^2 to 1000 W/m^2 with 200 W/m^2 steps while keeping the temperature constant at 298 K. On the other hand, Figure 4 shows the simulation results of the PV curves of the PV module under changing temperature while keeping the solar radiation constant at 1000 W/m^2.

Table 1: HIT-N220A01 PV module parameters.

Maximum power (P_{max})	220 W
Voltage at P_{max} (V_{mp})	42.7 V
Current at P_{max} (I_{mp})	5.17 A
Open circuit voltage (V_{oc})	52.3 V
Short circuit current (I_{sc})	5.65 A
Temperature coefficient of I_{sc}	1.98 mA/°C

2.2. DC-DC Isolated Ćuk Converter. DC conversion has gained the great importance in many applications, starting from low-power applications to high-power applications. Many DC-DC converter topologies have been developed. The well-known Ćuk converter is modified by inserting a current rectifier CR1 in series with the output resonant inductor L_r. In addition, a transformer operating at high frequency is inserted inside the DC-DC converter for isolation purposes and for voltage amplification, if needed. The isolated Ćuk converter is shown in Figure 5. The isolated Ćuk converter has fantastic features such as low and limited voltage stress on all switches over the entire duty ratio operating range from D = 0 to D = 1. Another feature is that isolated Ćuk converter eliminates both start-up and inrush current problems that isolated boost converter suffer from. In addition, the isolated Ćuk converter efficiency is high compared to the other isolated converters such as flyback converter, which suffers from low efficiency due to the voltage stresses on the output switch of the flyback converter, which could be many times higher than the regulated output voltage and hence finally leads to reduce the efficiency and

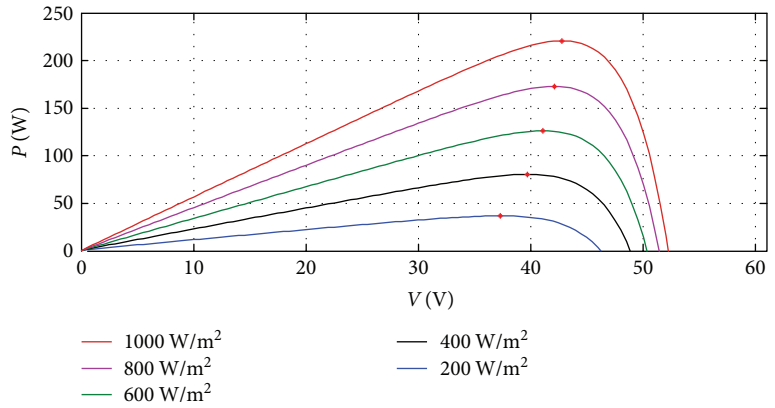

Figure 3: P-V curves under changing the solar radiation.

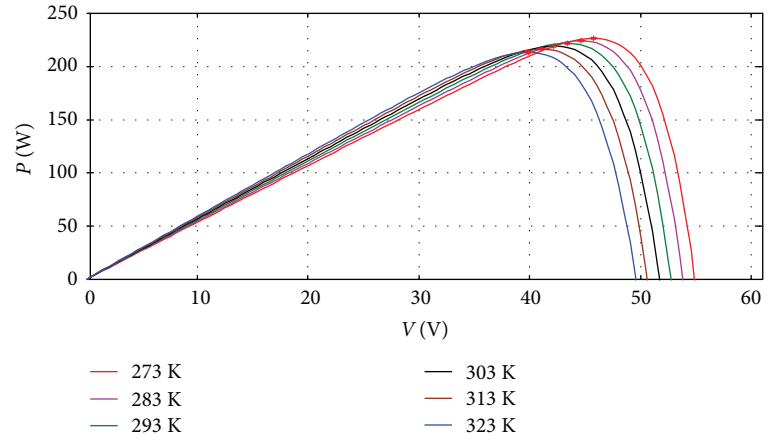

Figure 4: P-V curves under changing the temperature.

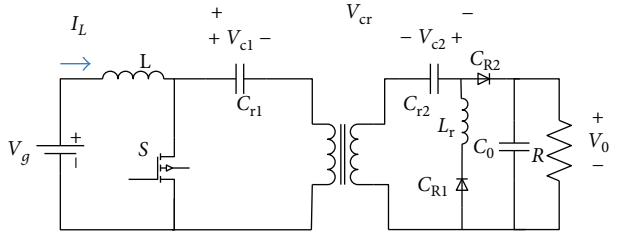

Figure 5: Isolated Ćuk Converter.

increase its cost. The isolated Ćuk converter has many attractive features, for more information refer to [27, 28].

The basic principle of the isolated Ćuk converter is that the MOSFET and the diode CR1 are working together during on state interval of the MOSFET. Only diode CR2 is working during MOSFET off state interval. The inductor voltage waveform, inductor current waveform, and the capacitor current waveform are shown in Figure 6. As shown in this figure, inductor voltage balance can be obtained as [27, 28]

$$V_g D + \left(V_g - V_{cr} - V_o\right) D' = 0. \tag{5}$$

During the full cycle in the resonance state, $V_{cr} = 0$; therefore,

$$V_g D + \left(V_g - V_o\right) D' = 0. \tag{6}$$

From (6), the output-to-input voltage ratio can be given as

$$M = \frac{V_o}{V_g} = \frac{1}{1 - D}, \tag{7}$$

where D is the duty cycle.

The above equation states that the output voltage will be boosted by changing the duty ratio. The polarity of the output voltage is the same as that of the input voltage.

In order to design the main inductor value, from the inductor voltage waveform in Figure 6, we get

$$\Delta_{iL} = \frac{V_g D T_s}{L}, \tag{8}$$

where T_s is the switching interval.

In addition, in order to design the output capacitor value, from the output capacitor current waveform in Figure 6, we get

$$\Delta V_{c0} = \left(-\frac{V_0}{R}\right) \frac{D T_s}{RC} = -\frac{V_g}{(1 - D)} \frac{D T_s}{RC}. \tag{9}$$

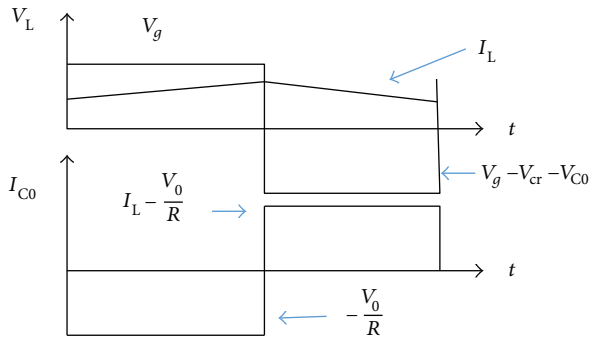

Figure 6: Waveforms of inductor voltage and capacitor current.

Table 2: Isolated Ćuk converter parameters.

Main inductor L	0.5 mH
Resonance inductor L_r	1.5 μH
Resonance capacitor $C_{r1} = C_{r2}$	20 μF
Capacitance C_{PV}	300 μF
Output capacitance C_o	33 μF
Switching frequency	30 KHz
Resistive load	35 Ω

According to the above equations, the design parameters of the isolated Ćuk converter are shown in Table 2.

3. The Proposed ANFIS-Based MPPT Method

In this paper, a new ANFIS-based MPPT method is proposed to achieve tracking the maximum power of the PV module under changing the weather conditions. The proposed input variables are the PV voltage (V_{PV}), PV current (I_{PV}), and the PV cell temperature (T_{PV}). The output variable is the duty cycle, which is used to control the DC-DC isolated Ćuk converter in order to keep tracking maximum power. Since the modeling of the conventional FLC is based on trial and error, the probability of obtaining the optimal performance is low. Therefore, obtaining membership functions and fuzzy rules can be done through learning using ANFIS. The trained data should be collected first. The following steps were executed in this paper to obtain the trained data:

(i) The system was simulated under different solar radiation and temperature conditions by using conventional MPPT algorithms.

(ii) The data were collected and manipulated using a MATLAB code, which is built for this purpose to get the desired data.

(iii) The manipulated data were then shuffled. The results data are then filtered again to obtain only the unique rows in collecting data. Finally, 60% of the resulting data are used for training and the remaining 40% are divided equally between testing and checking data.

The input trained data to the ANFIS are V_{PV}, I_{PV}, and T_{PV}. Figure 7 is the overall proposed ANFIS model structure, which is a five-layer network. Figure 8 is the membership function of the PV voltage (V_{PV}) generated by ANFIS. Figure 9 is the generated membership function of the PV current (I_{PV}) while Figure 10 is the generated membership functions of the PV cell temperature (T_{PV}). Each input has three generalized bell-shaped-type membership function named low, medium, and high. The output is the duty cycle, which is compared with the sawtooth signal in order to generate the suitable gate pulses for the Ćuk converter. The PV voltage varies from 36.49 V to 45.14 V, which is the area of the voltage at maximum power under different ambient conditions. On the other hand, the PV current varies from 2 A to 5.599 A, which is also the area of the current at maximum power under different ambient conditions. In addition, the PV cell temperature varies between 298 K and 323 K. The membership functions are generated by the ANFIS controller based on the prior knowledge obtained from the training dataset as described earlier. The membership function's shape varies during the training stage, and the final shape obtained after the completion of the training is shown in Figures 8, 9, and 10.

The rule base depicts the relationship and mapping between the input and output membership functions. One particular situation is shown in Figure 11 when V_{PV} is 39.5 V, I_{PV} is 3.51 A, and T_{PV} is 303 K. All the rules can be accessed by moving the red slider shown in Figure 11. Moving the slider results the output duty cycle of the ANFIS appearing in the last column of Figure 11, which is used to drive the MOSFET of the isolated Ćuk converter. As an example, rule 4 can be read as if V_{PV} is low, I_{PV} is medium and T_{PV} is low and then the duty cycle to achieve MPP is 0.33.

4. Experimental Setup

An experimental implementation setup was established to verify the performance of the proposed method practically. Figure 12 shows the schematic diagram of the hardware setup with the dSPACE 1104 board. Figure 13 shows the hardware setup of the MPPT system. In the hardware setup, one PV module model number HIT-N220A01 is connected to the DC-DC isolated Ćuk converter and then to the load. The isolated Ćuk parameters and the other parameters used in the hardware setup are listed in Table 2. The MOSFET type is IRFB4229 while the diode type is BYV32-200. Data acquisition and the control system are implemented by using dSPACE 1104 software and digital signal processor card on PC, respectively. In order to start the implementation, the PV voltage, the PV current, and the PV cell temperature must be initially measured. In this system, the PV voltage is measured by using the voltage divider while the PV current is measured by using hall effect current sensor model number LTS 25-NP. The measured signals are used to feed the ADC channels of the dSPACE board. On the other hand, the PV cell temperature is measured by using 10 KΩ negative temperature coefficient thermistor because it is inexpensive and simple. The thermistor is connected in series with a 10 KΩ

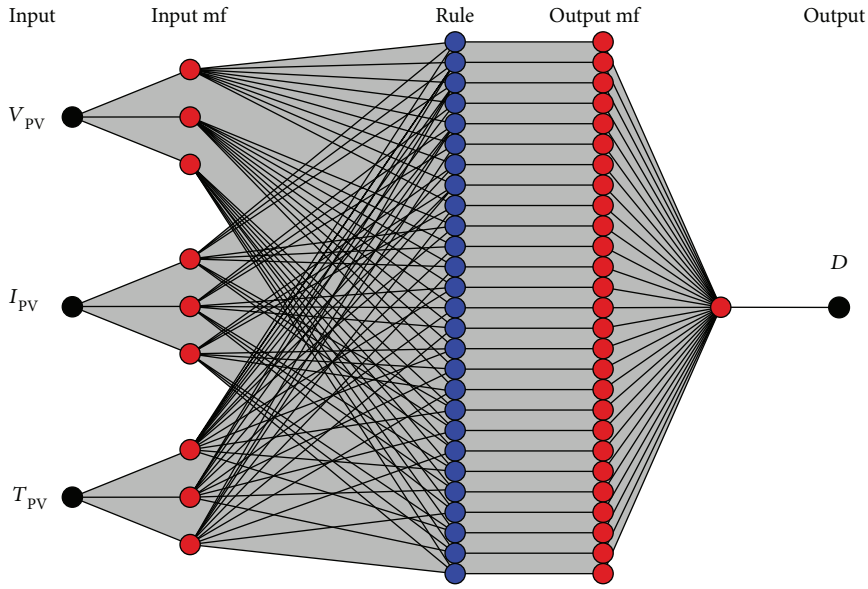

Figure 7: The proposed ANFIS model structure.

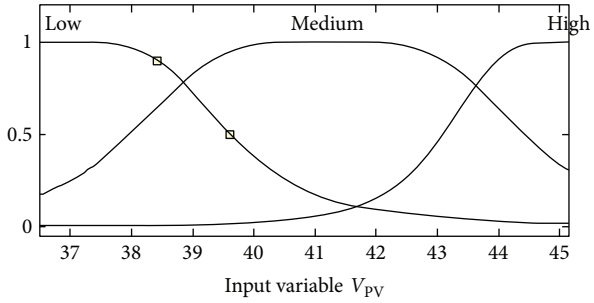

Figure 8: The membership function of the input variable (V_{PV}).

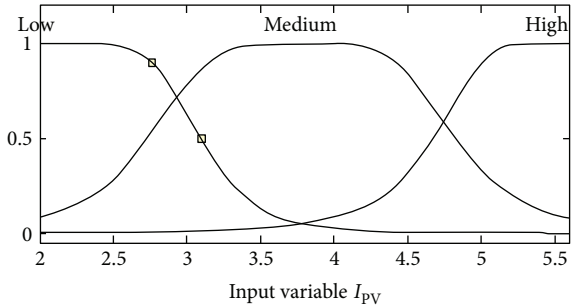

Figure 9: The membership function of the input variable (I_{PV}).

resistor to form a voltage divider fed by a 5 V voltage regulator. The voltage across the thermistor is used to feed the ADC channel of the dSPACE board. Inside SIMULINK, the low pass filters are used to remove undesired switching noises. The output signal of the MPPT algorithm is then applied to the PWM block, which is used to generate the required switching signal to drive the MOSFET. The PWM generated signal from the dSPACE is connected to the MOSFET of the Ćuk converter via optocoupler model number PS9505 as shown in Figure 12.

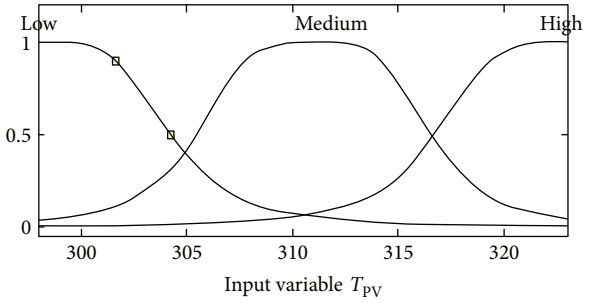

Figure 10: The membership function of the input variable (T_{PV}).

5. Simulation and Experimental Results

5.1. Simulation Results. The simulation is achieved using MATLAB/SIMULINK environment. The model used for simulation is shown in Figure 14. As shown in this figure, the input variables to the FLC are V_{PV}, I_{PV}, and T_{PV}. The output variable from the FLC is the duty cycle which is then compared with the sawtooth carrier signal. The result pulses are used to drive the MOSFET.

To verify the performance of the proposed MPPT method, three scenarios are applied to the proposed ANFIS-based MPPT method: constant weather condition scenario, dynamic weather condition scenario, and load variation scenario. For comparison purposes, the ANFIS-based MPPT method is compared with the conventional P&O MPPT method.

The PV module parameters used for simulation are shown in Table 1 while the other system parameters are shown in Table 2. The proposed ANFIS-based MPPT method is tested under the following scenarios.

5.1.1. Constant Weather Condition Scenario. A steady weather condition is realized by putting the solar radiation at 1000 W/m^2 and putting the PV temperature at 298 K.

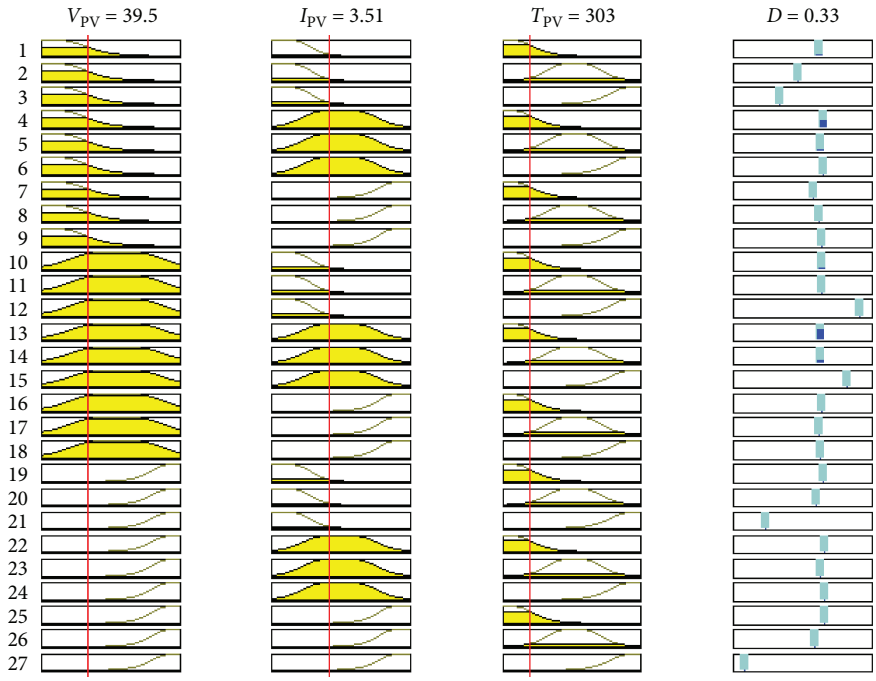

Figure 11: Rule base of ANFIS controller.

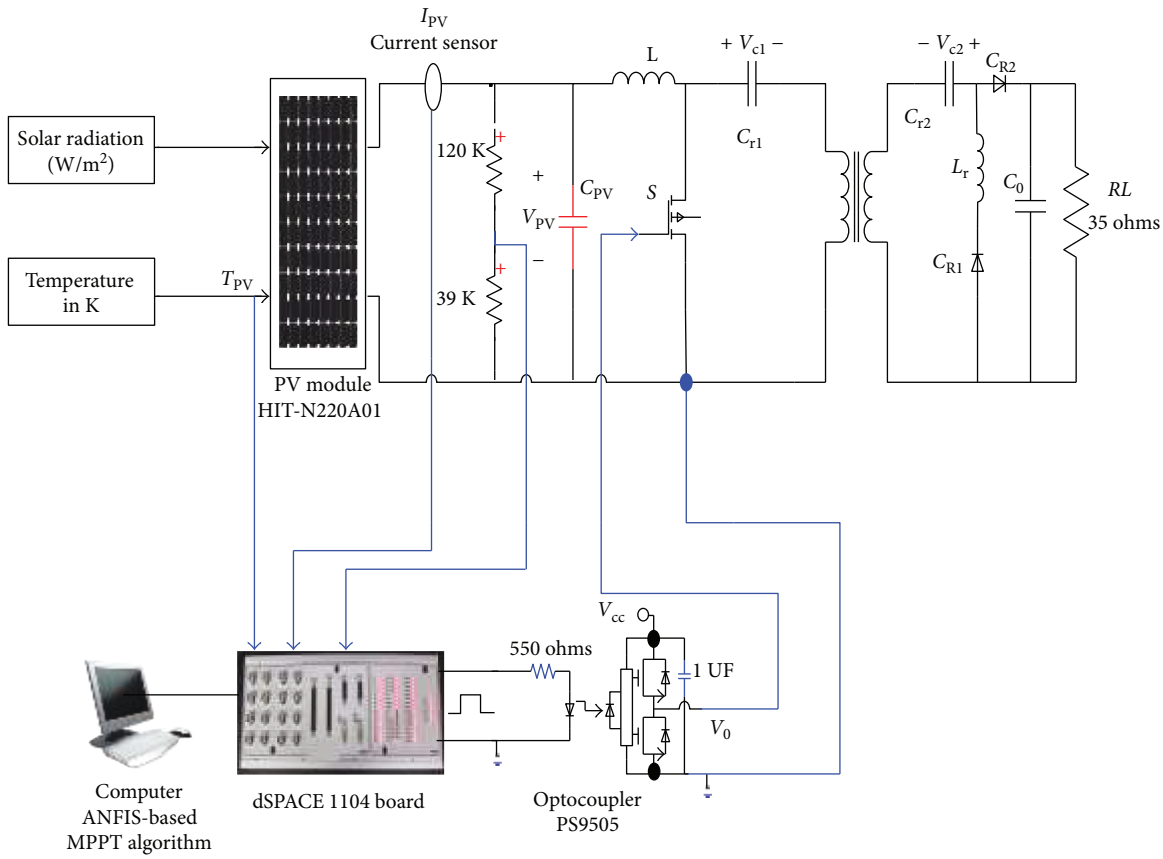

Figure 12: Schematic diagram of the hardware setup.

The ANFIS-based MPPT method succeeds in tracking the maximum power under the steady weather conditions as shown in Figure 15. In order to verify the effectiveness and the accuracy of the ANFIS-based MPPT method, its performance is compared with the conventional perturb and observe MPPT methods with two step sizes, 0.01 and 0.015.

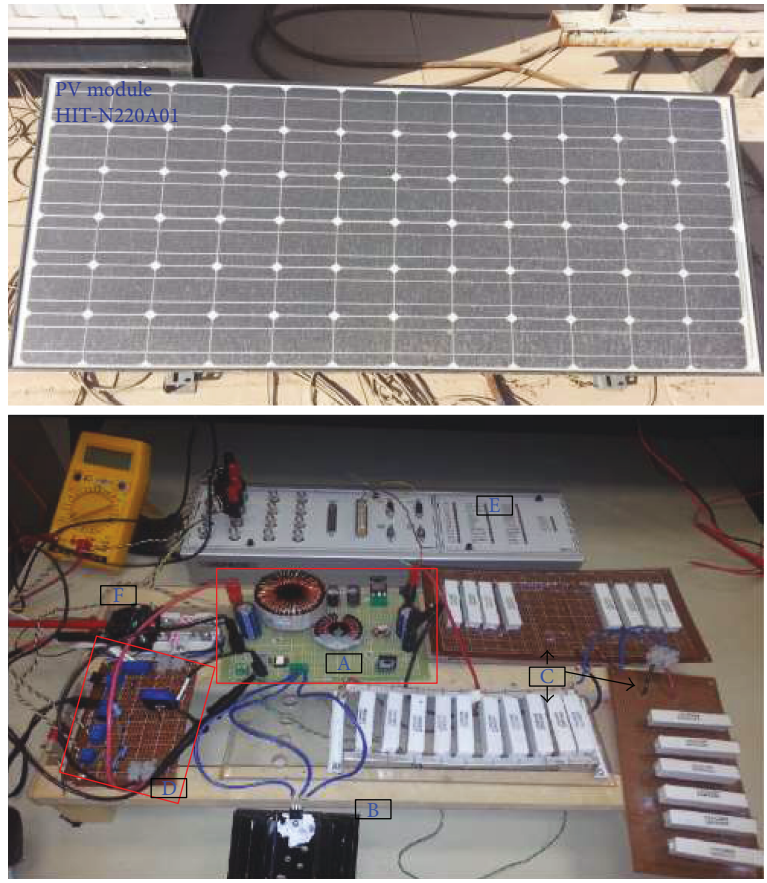

Figure 13: The hardware setup of the system. (a) DC-DC isolated Ćuk converter. (b) MOSFET model number IRFB4229 and its heat sink. (c) Resistive load bank. (d) Sensor board. (e) dSPACE 1104 board. (f) Input circuit breaker connected to the PV module.

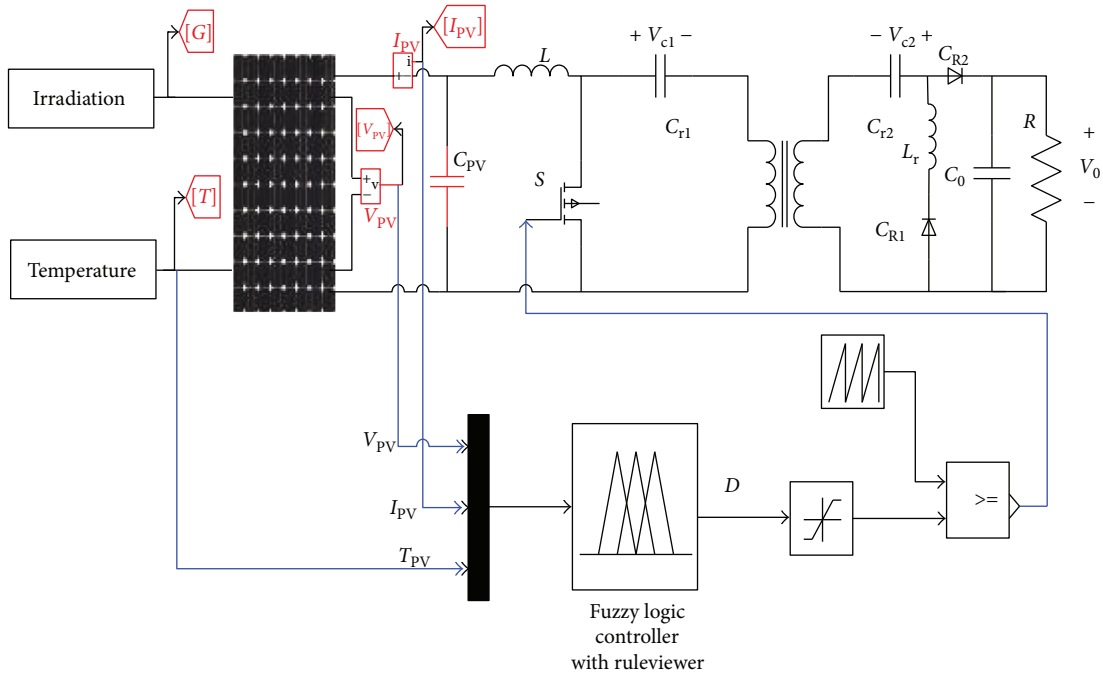

Figure 14: ANFIS-based MPPT system used for simulation.

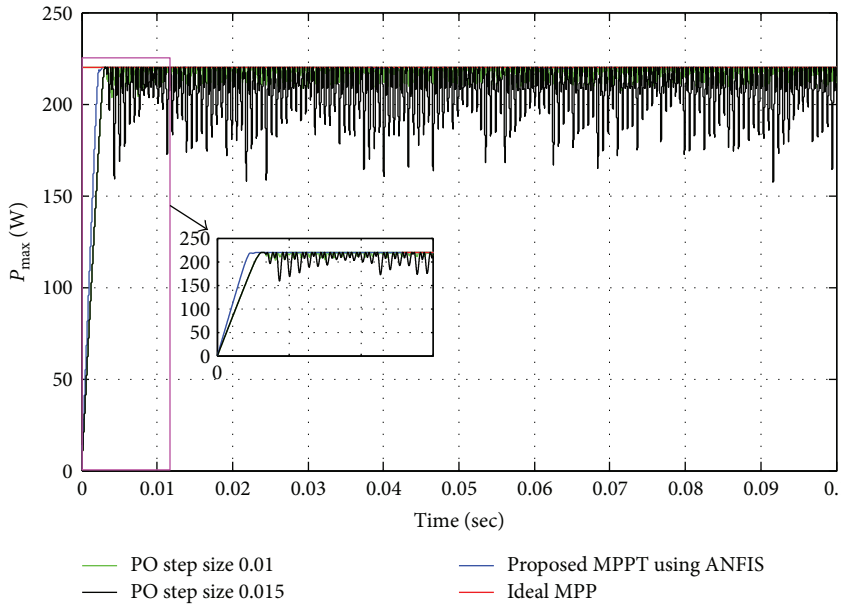

Figure 15: MPP tracking performance at constant weather conditions.

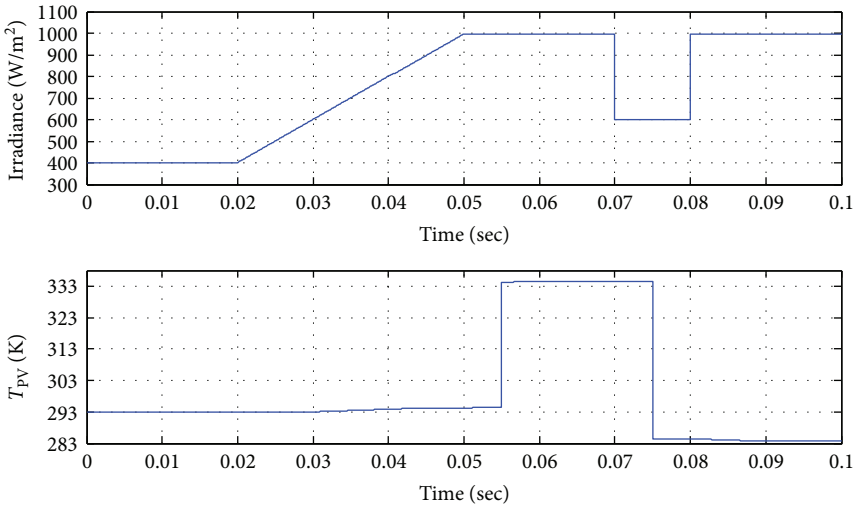

Figure 16: Changing the ambient condition.

As shown in Figure 15, the proposed method tracked the maximum power faster than the P&O method. In addition, the oscillations of the proposed method around maximum power point are lower compared to the P&O method at both step sizes. The percentage tracking efficiency for the MPPT can be given as

$$\eta = \frac{\int_{t_1}^{t_2} P_{\text{MPP}}\, dt}{\int_{t_1}^{t_2} P_{\text{ideal MPP}}\, dt}. \tag{10}$$

According to (10), by putting $t_1 = 0$ and $t_2 =$ end simulation time, the tracking efficiency of the proposed ANFIS-based MPPT method is calculated as 98.87%. On the other hand, the tracking efficiency of the P&O MPPT method at 0.01 step size is 97.34% while the tracking efficiency at 0.015 step size is 92.71%. In both cases, the tracking efficiency of the proposed method is higher.

5.1.2. Dynamic Weather Condition Scenario. In order to verify the accuracy of the proposed method under dynamic weather conditions, it is tested under the weather conditions shown in Figure 16. As shown in this figure, the solar radiation is kept constant at 400 W/m^2 until 0.02 sec. The solar radiation is then assumed to be changed as a ramp function with positive slope from 0.02 sec to 0.05 sec to account for changing the solar radiation in the sunrise periods. The irradiance is then changed as a unit step function to account for changing the solar radiation rapidly. On the other hand, the temperature is kept constant at 293 K until 0.03 sec. Then it is increased as a slope function. It is then stepped up to 334°F and then stepped down to 284 K.

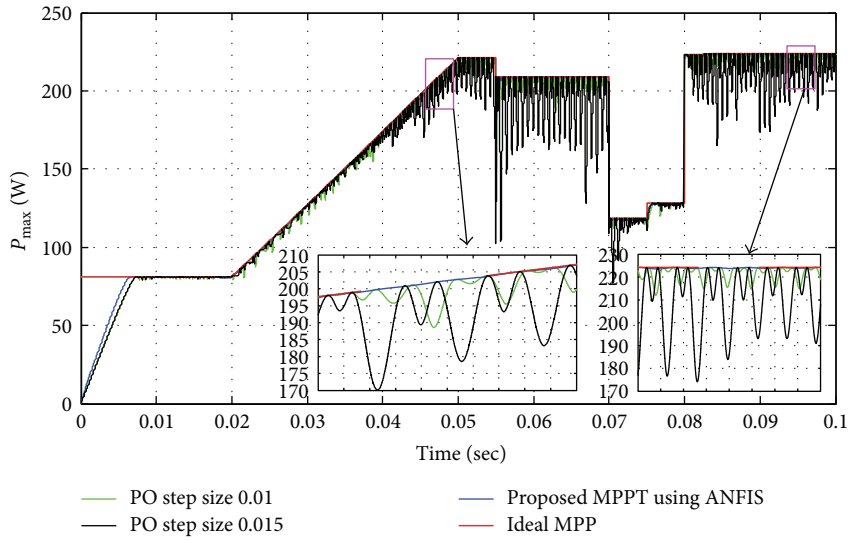

Figure 17: MPPT performance at dynamic weather conditions.

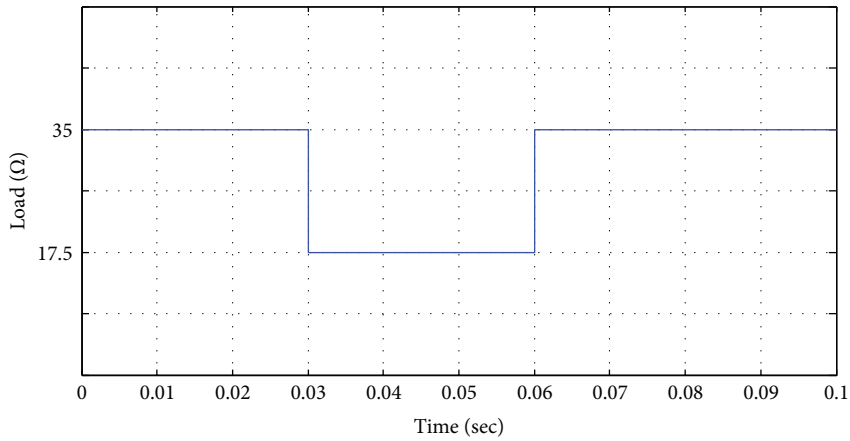

Figure 18: Load variation scenario.

The proposed method tracked the maximum power effectively and accurately under this dynamic weather conditions as shown in Figure 17. The proposed method is faster in tracking the MPP compared to the P&O MPPT method at both step sizes, 0.01 and 0.015. In addition, the oscillations around MPP are lower than the oscillations caused by the P&O MPPT method at both step sizes. According to (10), the tracking efficiency of the proposed method under this dynamic weather conditions is about 98.34%, which is higher than the tracking efficiency of the P&O MPPT at both step sizes. The tracking efficiency of the P&O MPPT at 0.01 step size is 96.93% while the tracking efficiency at 0.015 step size is 93.89%.

5.1.3. Load Variation Scenario. To extra prove the effectiveness and robustness of the proposed MPPT method, the proposed method is tested under load variations. The load is changed as shown in Figure 18 while keeping the weather conditions constant at 1000 W/m^2 and 298°F. As shown in this figure, the load is kept constant at 35 Ω unit 0.03 sec, at which the load is reduced to 17.5 Ω. The load is then again changed to 35 Ω at 0.06 sec. Figure 19 shows the maximum power tracked by the proposed ANFIS-based MPPT as well as the power tracked by the P&O method. As shown in this figure, the proposed method tracked the maximum power accurately under changing load. It is clear that the ANFIS-based MPPT method is robust under changing loads compared to the performance of the P&O method.

From above simulation results, Table 3 concludes the comparison between the proposed ANFIS-based MPPT method and the P&O MPPT method. Both methods need voltage and current measurements of the PV module. Only ANFIS-based MPPT method needs temperature measurements as an extra input. It is evident from simulation results that the tracking speed of the ANFIS-based MPPT method is faster. In addition, oscillations around MPP are smaller compared to the P&O MPPT method since P&O MPPT method suffers from high oscillations around MPP, which depend on step size. On the other hand, ANFIS-based MPPT method is more robust compared to P&O method. It is also evident

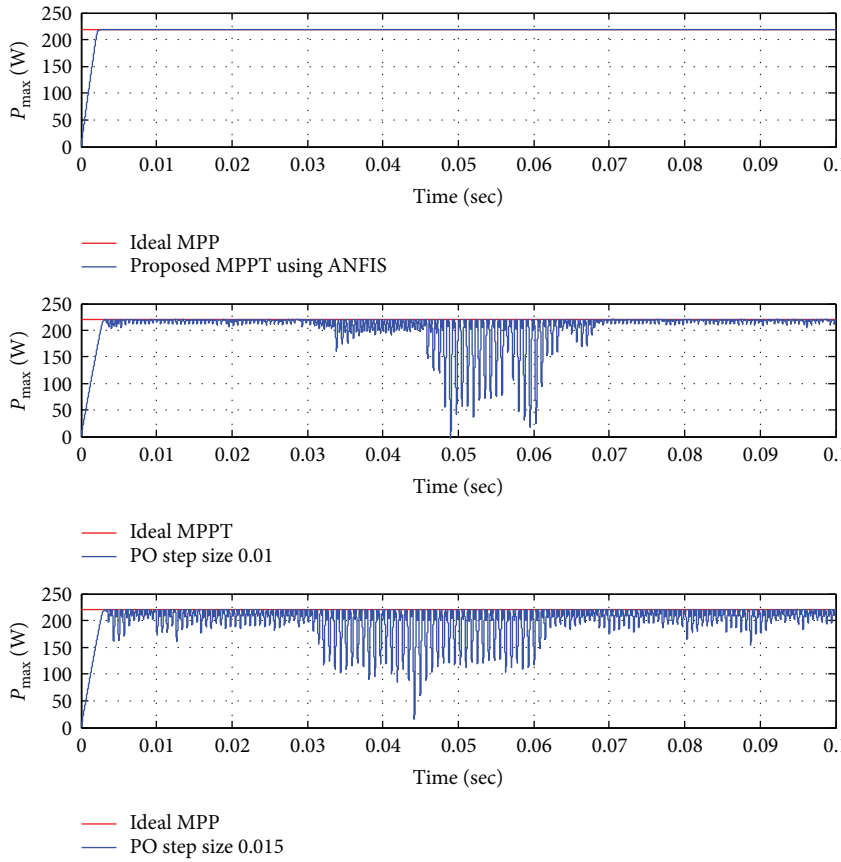

Figure 19: MPP tracking performance under load changes.

Table 3: Comparison of proposed MPPT and P&O MPPT methods.

	Proposed ANFIS-based MPPT method	Conventional P&O MPPT method
PV current measurements	Yes	Yes
PV voltage measurements	Yes	Yes
PV temperature measurements	Yes	No
Tracking speed	High	Depends on step size
PV panel dependency	Yes	No
Robustness	High	Medium
Oscillations around MPP	Less	Depends on step size
Tracking efficiency	High	Medium

from simulation results that the tracking efficiency of the ANFIS-based MPPT method is higher than the efficiency of the P&O MPPT method.

5.2. Experimental Results. To verify the function and the performance of the proposed ANFIS-based MPPT method, a 220 W prototype is built and the proposed method is experimentally tested with the help of dSPACE 1104 data acquisition system. In order to show the performance of the ANFIS-based method, the method is tested on a sunny day as well as on a cloudy day to prove the effective tracking performance under all weather conditions.

5.2.1. Sunny Day. Steady weather conditions practically mean testing the proposed method on a sunny day. Figure 20 shows the changing solar radiation and the PV cell temperature, which are measured from 9:23 AM until 3:00 PM on a sunny day. Figure 21 shows the maximum power tracked by using the proposed method. The PV voltage at MPP, PV current at MPP, and the duty cycle measured from the output of the FLC are also shown in Figure 21. As shown in this figure, the proposed method has tracked the maximum power successfully and accurately.

5.2.2. Cloudy Day. Having a depth investigation on the behavior of the proposed MPPT system under dynamic weather conditions, the proposed method is tested under the weather conditions shown in Figure 22. As shown in Figure 22, the changing solar radiation and the PV cell temperature are measured from 12:56 PM until 3:00 PM on a cloudy day. The proposed method is tested under this weather condition. Variations of the tracked power, PV voltage at MPP, PV current at MPP, and the duty cycle are shown

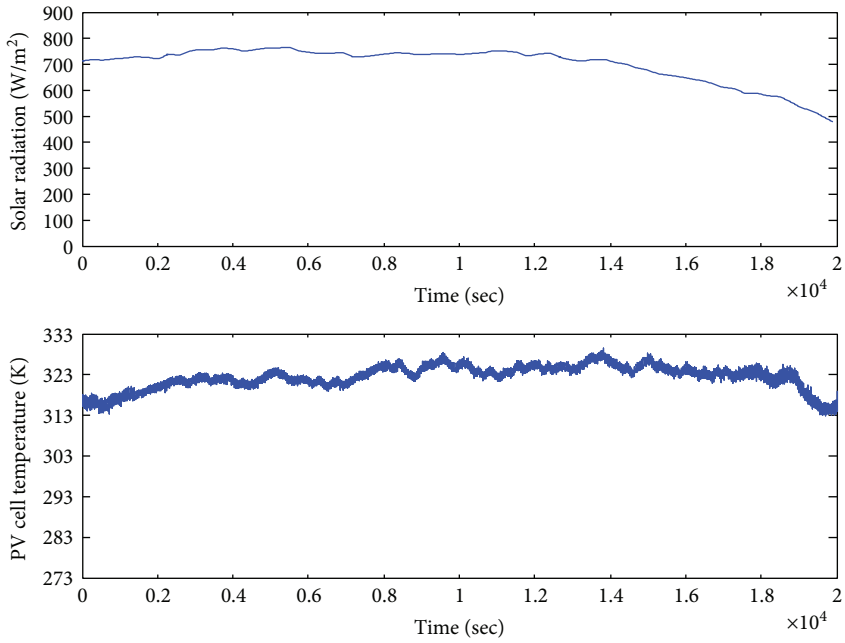

Figure 20: Changing the solar radiation and PV temperature on a sunny day. From 9:23 AM to 3:00 PM.

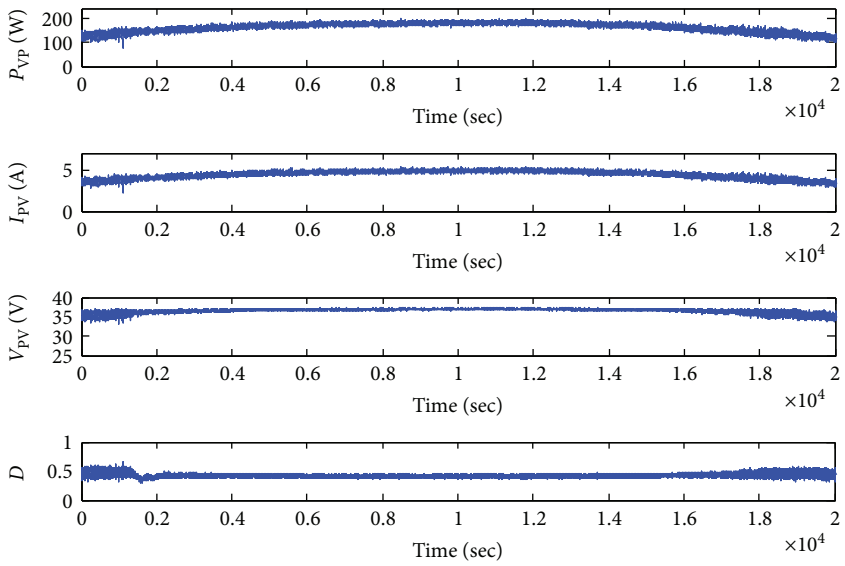

Figure 21: Experimentally tracking behavior of the ANFIS MPPT. From 9:23 AM to 3:00 PM.

in Figure 23. As shown in this figure, the proposed method has tracked the maximum power effectively and accurately under dynamic solar radiation.

6. Conclusion

Photovoltaic model using MATLAB/SIMULINK and the design of appropriate DC-DC isolated Ćuk converter with a maximum power point tracking facility are presented in this paper. ANFIS-based MPPT method is proposed in this paper and simulated using MATLAB/SIMULINK environment. The proposed method is tested under disturbances in the weather conditions to show its tracking performance. The tracking behavior shows that the proposed MPPT method successfully and accurately tracked the maximum power under all scenarios with higher efficiency and lower oscillations around MPP compared to the conventional P&O MPPT method. The comparison of the proposed method and conventional P&O MPPT method is also presented in the simulation results. The experimental implementation of the proposed ANFIS-based MPPT method is done in this paper. Data acquisition and the control of the proposed ANFIS-based MPPT method are done by dSPACE 1104 software and digital signal processor card on PC, respectively. The experimental results show how the proposed method tracked the MPP effectively and

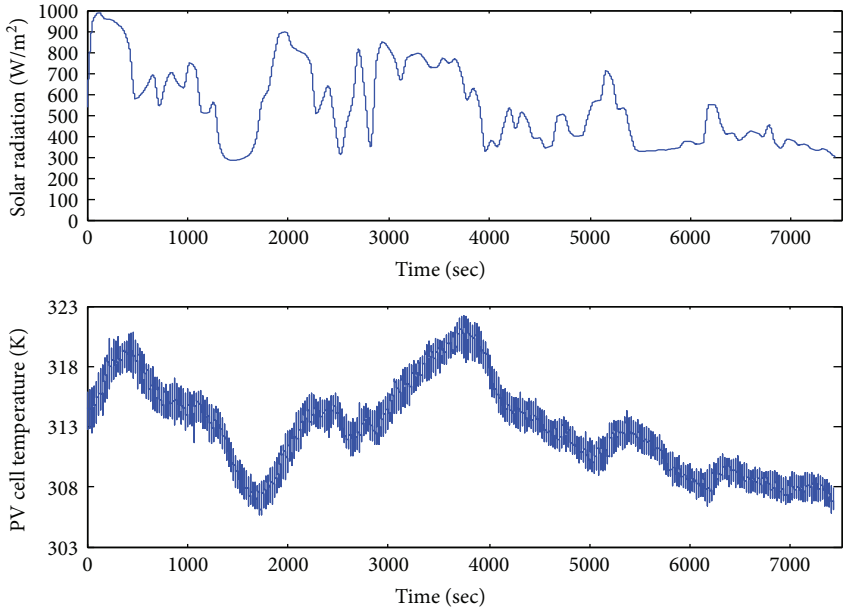

Figure 22: Changing the solar radiation and PV temperature on a cloudy day. From 12:56 PM to 3:00 PM.

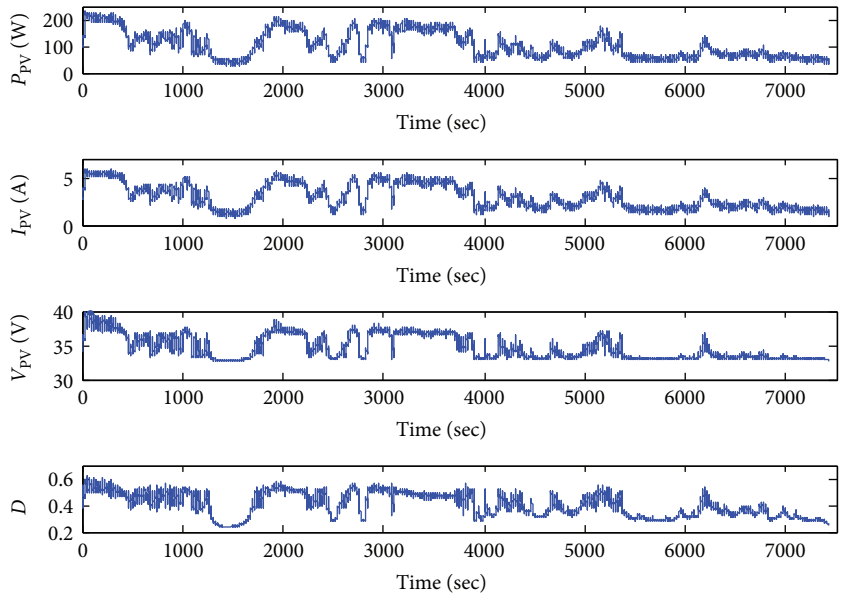

Figure 23: Experimentally tracking behavior of the ANFIS MPPT. From 12:56 PM to 3:00 PM.

accurately with fast response and low oscillations. The ANFIS-based MPPT method is well functioning under practical steady and dynamic weather condition. This method is effectively capable of improving maximum power tracking of PV modules.

Conflicts of Interest

The authors assure that the authors of this manuscript do not have any interest in dSPACE 1104 board and its software. The authors used dSPACE 1104 for research purpose only without any relations with the manufacturer or dealer.

Acknowledgments

The authors would like to acknowledge the support provided by the Deanship of Scientific Research at King Saud University, through the Research Centre at the College of Engineering.

References

[1] T. C. Yu and T. S. Chien, "Analysis and simulation of characteristics and maximum power point tracking for photovoltaic systems," in *International Conference on Power Electronics and Drive Systems (PEDS)*, pp. 1339–1344, Taipei, Taiwan, November 2009.

[2] J. L. Santos, F. Antunes, A. Chehab, and C. Cruz, "A maximum power point tracker for PV systems using a high performance boost converter," *Solar Energy*, vol. 80, no. 7, pp. 772–778, 2006.

[3] D. Hohm and M. Ropp, "Comparative study of maximum power point tracking algorithms using an experimental, programmable, maximum power point tracking test bed," in *Conference Record of the Twenty-Eighth IEEE Photovoltaic Specialists Conference*, pp. 1699–1702, Anchorage, AK, USA, September 2000.

[4] T. Esram and P. L. Chapman, "Comparison of photovoltaic array maximum power point tracking techniques," *IEEE Transactions on Energy Conversion*, vol. 22, no. 2, pp. 439–449, 2007.

[5] V. Salas, E. Olias, A. Barrado, and A. Lazaro, "Review of the maximum power point tracking algorithms for stand-alone photovoltaic systems," *Solar Energy Materials and Solar Cells*, vol. 90, no. 11, pp. 1555–1578, 2006.

[6] A. N. A. Ali, M. H. Saied, M. Mostafa, and T. Abdel-Moneim, "A survey of maximum PPT techniques of PV systems," in *Energytech, 2012 IEEE*, pp. 1–17, Cleveland, OH, USA, May 2012.

[7] A. M. Z. Alabedin, E. El-Saadany, and M. Salama, "Maximum power point tracking for photovoltaic systems using fuzzy logic and artificial neural networks," in *2011 IEEE Power and Energy Society General Meeting*, pp. 1–9, Detroit, MI, USA, July 2011.

[8] C. Larbes, S. M. Aït Cheikh, T. Obeidi, and A. Zerguerras, "Genetic algorithms optimized fuzzy logic control for the maximum power point tracking in photovoltaic system," *Renewable Energy*, vol. 34, no. 10, pp. 2093–2100, 2009.

[9] C. A. P. Tavares, K. T. F. Leite, W. I. Suemitsu, and M. D. Bellar, "Performance evaluation of photovoltaic solar system with different MPPT methods," in *35th Annual Conference of IEEE Industrial Electronics*, pp. 719–724, Porto, Portugal, November 2009.

[10] J. Li and H. Wang, "Maximum power point tracking of photovoltaic generation based on the fuzzy control method," in *International Conference on Sustainable Power Generation and Supply*, pp. 1–6, Nanjing, China, April 2009.

[11] F. Chekired, C. Larbes, D. Rekioua, and F. Haddad, "Implementation of a MPPT fuzzy controller for photovoltaic systems on FPGA circuit," *Energy Procedia*, vol. 6, pp. 541–549, 2011.

[12] M. Adly, H. El-Sherif, and M. Ibrahim, "Maximum power point tracker for a PV cell using a fuzzy agent adapted by the fractional open circuit voltage technique," in *2011 IEEE International Conference on Fuzzy Systems (FUZZ)*, pp. 1918–1922, Taipei, Taiwan, June 2011.

[13] M. A. Islam, A. Talukdar, N. Mohammad, and P. K. S. Khan, "Maximum power point tracking of photovoltaic arrays in Matlab using fuzzy logic controller," in *Annual IEEE India Conference (INDICON)*, pp. 1–4, Kolkata, India, December 2010.

[14] M. S. Ngan and C. W. Tan, "A study of maximum power point tracking algorithms for stand-alone photovoltaic systems," in *2011 IEEE Applied Power Electronics Colloquium (IAPEC)*, pp. 22–27, Johor Bahru, Malaysia, April 2011.

[15] I. Purnama, Y. K. Lo, and H. J. Chiu, "A fuzzy control maximum power point tracking photovoltaic system," in *IEEE International Conference on Fuzzy Systems (FUZZ)*, pp. 2432–2439, Taipei, Taiwan, June 2011.

[16] Y. H. Chang and W. F. Hsu, "A maximum power point tracking of PV system by adaptive fuzzy logic control," in *International MultiConference of Engineers and Computer scientists*, Hong Kong, March 2011.

[17] A. M. Noman, K. E. Addoweesh, and H. M. Mashaly, "A fuzzy logic control method for MPPT of PV systems," in *IECON 2012-38th Annual Conference on IEEE Industrial Electronics Society*, pp. 874–880, Montreal, QC, Canada, October 2012.

[18] T. A. Ocran, J. Cao, B. Cao, and X. Sun, "Artificial neural network maximum power point tracker for solar electric vehicle," *Tsinghua Science and Technology*, vol. 10, no. 2, pp. 204–208, 2005.

[19] R. Ramaprabha and B. Mathur, "Intelligent controller based maximum power point tracking for solar PV system," *International Journal of Computer Applications*, vol. 12, no. 10, pp. 37–42, 2011.

[20] N. Khaehintung, P. Sirisuk, and W. Kurutach, "A novel ANFIS controller for maximum power point tracking in photovoltaic systems," in *The Fifth International Conference on Power Electronics and Drive Systems, 2003. PEDS 2003*, pp. 833–836, Singapore, Singapore, November 2003.

[21] R. A. Majin, A. Gharaveisi, J. Khorasani, and M. Ahmadi, "Speed improvement of MPPT in photovoltaic systems by fuzzy controller and ANFIS reference model," *System*, vol. 1, p. 4, 2006.

[22] A. M. S. Aldobhani, "Maximum power point tracking of PV system using ANFIS prediction and fuzzy logic tracking," in *Proceedings of the International MultiConference of Engineers and Computer Scientists*, Hongkong, March 2008.

[23] C. A. Otieno, G. N. Nyakoe, and C. W. Wekesa, "A neural fuzzy based maximum power point tracker for a photovoltaic system," in *AFRICON, 2009. AFRICON'09*, pp. 1–6, Nairobi, Kenya, September 2009.

[24] H. Abu-Rub, A. Iqbal, S. M. Ahmed, F. Z. Peng, Y. Li, and G. Baoming, "Quasi-Z-source inverter-based photovoltaic generation system with maximum power tracking control using ANFIS," *IEEE Transactions on Sustainable Energy*, vol. 4, no. 1, pp. 11–20, 2013.

[25] M. G. Villalva and J. R. Gazoli, "Modeling and circuit-based simulation of photovoltaic arrays," in *Power Electronics Conference*, pp. 1244–1254, Bonito-Mato Grosso do Sul, Brazil, October 2009.

[26] G. Walker, "Evaluating MPPT converter topologies using a MATLAB PV model," *Australian Journal of Electrical & Electronics Engineering*, vol. 21, no. 1, pp. 49–56, 2001.

[27] S. Cuk and Z. Zhang, "Voltage step-up switching DC-to-DC converter field of the invention," 2010, U.S. Patent 7 778 046.

[28] S. Cuk, "Single-stage, AC-DC converter topologies of 98% efficient single phase and three-phase rectifiers," in *Keynote Paper at Power Conversion and Intelligent Motion (PCIM) Europe*, 2011.